Polymer Chemistry

Accepted Manuscript

ROYAL SOCIETY OF CHEMISTRY

www.rsc.org/polymers

A Rapid Crosslinking Injectable Hydrogel for Stem Cell Delivery, from Multifunctional Hyperbranched Polymers via RAFT Homopolymerization of PEGDA

Yixiao Dong[1.2*], Yue Qin[1], Marie Dubaa[1], John Killion[3], Yongsheng Gao[1], Tianyu Zhao[1], Dezhong Zhou[1], Dominik Duscher[2], Luke Geever[3], Geoffrey C. Gurtner[2] and Wenxin Wang[1*]

[1] The Charles Institute of Dermatology, School of Medicine and Medical Science, University College Dublin, Dublin, Ireland.
E-mail: wenxin.wang@ucd.ie

[2] Stanford University School of Medicine, Stanford, CA, United States.

E-mail: yixiaod@stanford.edu

[3] Applied Polymer Technology, Athlone Institute of Technology, Athlone, Ireland.

[*] Corresponding authors.

KEYWORDS: Injectable Hydrogel, Adipose Tissue-Derived Stem Cells, RAFT, Divinyl Monomer, Hyperbranched Polymers

ABSTRACT: Stem cell therapies have been attracted much attention for the last few decades in the field of regenerative medicine and tissue engineering. 3-dimensional (3D) microenvironment surrounding the transplanted stem cells plays essential roles that influence the cell fate and behaviors. Thus advanced functional biomaterials and extracellular matrix (ECM) replacements with adjustable chemical, mechanical and bioactive properties are requisite in this field. In this study, PEG-based hyperbranched multifunctional homopolymers were developed via RAFT homopolymerization of the divinyl monomer of poly(ethylene glycol) diacrylate (PEGDA). Due to its high degree of multi-acrylate functionality, the hyperbranched polyPEGDA can rapidly crosslink with a thiolated hyaluronic acid at physiological condition and form an injectable hydrogel for cell delivery. In addition, by simply varying the synthesis recipe such as the reaction time and the ratio of the monomer to chain transfer agent (CTA), tunable polymer molecular weight, acrylate functionality degree and the cyclized/hyperbranched polymeric architecture can be finely controlled in one-step reaction. The gelation speed and the mechanical properties of this hydrogel can be easily adjusted by altering the crosslinking conditions. Rat adipose-derived stem cells (rASC) were embedded into the in situ crosslinked hydrogels, and their cellular behavior such as the morphology, viability, metabolic activity and proliferation were fully evaluated. The results suggested the hydrogel maintained good cell viability and be able to easily modify with other bioactive signals, which provide this injectable hydrogel delivery system a decent potential for polymeric biomaterial and tissue regeneration applications.

Introduction

Cell based therapies, especially stem cell therapies have been attracted much attention for the last few decades in the field of regenerative medicine and tissue engineering. Increased evidence indicates that the traditional 2-dimensional (2D) cell culture systems cannot fully mimic the natural tissue microenvironment, thus advanced 3-dimensional (3D) extracellular matrix (ECM) replacements are required not only for developing our understanding on stem cell behavior, but also for the potential applications of the stem cell therapies in clinics [1-3]. To this end, hydrogels, as a 3D water-content network have been mostly studied because of their resemblance to the natural tissue such as porosity, permeability and similar mechanical properties. Compared to the hydrogels from the natural biomaterials (e.g. collagen, fibrin, alginate, chitosan, hyaluronic acid (HA) etc.), the synthetic polymers display remarkable advantages such as the convenient control on material composition and hydrogel architecture, the flexible physical and mechanical properties, and the capability to be tailored or modified with specific bioactive functions [4, 5].

Poly(ethylene glycol) (PEG) is one of the most widely studied synthetic polymers in the field due to its outstanding benefits including non-immunogenicity and resistance to protein adsorption [6, 7]. However, PEG-based hydrogels usually display minimal or no biological functionality due to their non-adhesive and non-degradable nature. Much effort has been devoted to develop the bioactive modified PEG-based hydrogels to mimic the natural ECM environment, but to actualize these modifications, multi-step modified reactions and purification are usually required for adding the functional group on the polymers [8-11]. Previously, series of PEG-based hydrogel systems have been developed in our group, from the hyperbranched multifunctional copolymers via one-step controlled living polymerization approaches (e.g. in-situ Deactivation Enhanced - Atom Transfer Radical Polymerization (in-situ DE-ATRP) and Reversible Addition

Fragmentation Chain Transfer (RAFT)) [12-14]. High level of vinyl functionality was achieved by introducing large amount of divinyl monomers, which provided these copolymers advanced capability of in situ gelation either via photo-initiated polymerization or chemically crosslinking with thiol-functional biomolecules (e.g. thiolated HA). Compared with commercially available PEG-based vinyl functional monomers (e.g. poly(ethylene glycol) diacrylate (PEGDA)) or polymers (e.g. 4-arm-PEG-Acr), our copolymers exhibit extraordinary advantages such as adjustable vinyl content, rapid gelation capability, well-controlled polymer structure and simple preparation via a one-step reaction.

However, the copolymerization of monovinyl and divinyl monomers, as in our previous works, still restricted the vinyl content level in the final products, and complicated the synthesis and purification procedure at some level. In this study, more active multifunctional homopolymers were developed via one-step RAFT homopolymerization of the divinyl monomer of PEGDA. The chain transfer agent (CTA) significantly delayed the reaction gelation and different polymer molecular weight, vinyl content, and polymeric architecture of the intramolecular cyclization and the intermolecular coupling can be finely controlled by varying the reaction time and the ratio of the monomer to the CTA. Based on these homopolymers, injectable hydrogels with flexible gelation and mechanical properties were developed via crosslinking with the commercially available thiolated HA. The rapid chemical gelation can be achieved within one to five minutes due to the high degree of multi-acrylate functionality of these homopolymers. In addition, rat adipose-derived stem cells (rASC) were embedded into the controlled 3D hydrogel environment in vitro, and the cell morphology, viability, metabolic activity and proliferation were fully evaluated up to two weeks. The results suggested the hydrogel maintained good cell viability and

be able to easily modify with other bioactive signals, which provide this injectable hydrogel system a decent potential for stem cell culture and delivery in tissue regeneration applications.

Results and Discussion

Synthesis of Hyperbranched polyPEGDA via RAFT Homopolymerization

The highly branched, or hyperbranched polymers exhibit much different physical properties and advantages comparing to their linear analogues such as low intrinsic viscosity, dense accessible end points (or functional groups), plus unique phase separation and surface behaviors [15-18]. Polycondensation of AB_n type monomers and self-condensing vinyl polymerization (SCVP) of inimers have been widely applied to synthesis the hyperbranched polymers [19-23]. Recently, increased attention has been paid to the synthesis of hyperbranched polymers by controlled/living polymerization such as ATRP and RAFT approaches. However, in the most of these studies, either only small amount of the divinyl monomers were copolymerized with monovinyl monomers (also known as "Strathclyde synthesis" method), or homopolymerization of divinyl monomers in the dilute conditions, lead to increased intramolecular cyclization and reduced number of the pendant vinyl functional groups in the final products [24-29].

In the present study, PEG-based hyperbranched homopolymers with abundant of pendant vinyl functional groups were synthesized by RAFT homopolymerization of poly(ethylene glycol) diacrylate (PEGDA, M_n = 575 g/mol) at a relatively high monomer concentration, where 2,2′-Azobis(2-methylpropionitrile) (AIBN) was used as an reaction initiator and 2-cyanoprop-2-yl dithiobenzoate was used as the chain transfer agent (CTA) as shown in **Scheme 1A**. Different ratio of PEGDA monomer to CTA ($[M]_0$:$[CTA]_0$ = 100/50/25:1) were used to adjust the

molecular architecture of the polymers, with consistent monomer concentration ([M] = 0.4 mol/L) and CTA:AIBN ratio (2:1). All reactions were performed at 60 ^{o}C.

The reactions were monitored by gel permeation chromatography (GPC) analysis and were stopped once the polydispersity index (PDI) of the polyPEGDA increased significantly, which indicated the intermolecular chain couplings occur [30]. The results were summarized in **Table 1**. In this system, because of the nature of the divinyl monomers, the active propagating radicals can react with either the free monomer or the pendant vinyl groups on the polymer chain, which leads to different polymerization behaviors and polymeric architectures. The polymer chain propagation and branching can be detected by GPC trace (**Figure 1**). At the beginning phase of the reaction, polymer chain propagation occupied the major role due to the high concentration of the unreacted monomers, leading to the linear polymeric chain with pendant vinyl groups. Along with the reaction proceeding, the local concentration of the pendant vinyl group increased and the more flexible longer polymer chain structure increased the possibility of forming the intramolecular cyclization. The intramolecular cyclization would not dramatically change the molecular weight of the polymer chains, therefore at this stage, the GPC traces shows a symmetrical peak with relatively narrow PDI. In contrast, at the later stage, larger polymeric molecules formed with the reduced free monomer distribution, meantime the intermolecular chain coupling are more likely occurring than the propagation which led to a broad multimodal peak with dramatically increasing on the overall molecular weight and PDI. It is worth to notice that the determination of the molecular weight of the hyperbranched polymer is based on a given linear polymer standard (i.e. PMMA) which will cause the ineluctable erroneous results. To overcome this problem, in this study, the samples were also characterized by a viscosity detector with universal calibration principle. It was shown that the number average molecular weights

(M_n) determined by GPC/viscosity were higher than conventional GPC/RI detection, and this difference became more obvious in the later stage of the reaction (**Table 1**). In addition, the Mark-Houwink constant (α) is commonly used for defining the relationship between polymer solution viscosity and molecular weights. Typically, whose α value between 0.2 and 0.5 can be considered as a spherical conformation of the branched system, and linear homopolymers usually exhibit α value between 0.6 and 0.8 because of the random coil conformation [29]. In this study, the Mark-Houwink exponents retaining around 0.2-0.3 suggested the branched structures of the polyPEGDA homopolymers (**Table 1**).

Effect of Monomer/CTA Ratio on Adjustable Polymeric Architecture

For the purpose of controlling the molecular weight and the polymeric architecture, different $[M]_0$:$[CTA]_0$ ratio (25/50/100:1) were carried out in this study. As expected, the molecular weights of the polyPEGDA increased by the rising $[M]_0$:$[CTA]_0$ ratio with the same reaction time. For example, the M_n increased from 6 kg/mol ($[M]_0$:$[CTA]_0$ = 25:1) to 35 kg/mol ($[M]_0$:$[CTA]_0$ = 100:1) at the 4.5 h (**Table 1**). However, the rate of the polymerization shows quite similar but with slightly reduction with the lower monomer/CTA ratio (**Figure 2A-B**). We believed this reduction was caused by the increased possibility of the radical chain transfer and termination at the lower monomer/CTA ratio condition due to the higher chain/radicals density in small regions. It has been reported that the increased RAFT agent can significantly postpone the gel point [31-33]. Here, with the higher monomer/CTA ratio condition ($[M]_0$:$[CTA]_0$ = 100:1), the molecular weight and distribution dramatically increased at the later reaction phase leading to the earlier gelation; in contrast this trend was significantly delayed with the lower monomer/CTA ratio (or in other words, with higher concentration of the RAFT agent) (**Figure 2C-D**), which was consistent with the former studies. The branched structure and the pendent

acrylate groups of the hyperbranched polyPEGDA were analyzed by ^{1}H NMR. The pendent acrylate groups were identified as three characteristic chemical shifts of 6.4 to 5.8 ppm (**Figure 3**). With the reaction proceeding, the pendent acrylate groups were expended by intramolecular cyclization and intermolecular coupling in all reactions (**Table 1**). Higher monomer/CTA ratio led to remarkable higher branching degree (or lower pendent acrylate level) per polymer chain at certain monomer conversion ratio since the initial stage of the polymerization (**Figure 4**). As discussed earlier, the intramolecular cyclization played major role versus intermolecular coupling at the early stage of the reaction, thus the results indicated that the higher monomer/CTA ratio increased the intramolecular cyclization. However, the slope of the curves from the different conditions kept consistent, which indicated that the monomer/CTA ratio did not influence the kinetic nature of the competition between polymer chain linear propagation and intra/inter-molecular branching. In other words, the overall rates of expending the pendant vinyl groups were same among different groups. Instead, other factors have been reported to affect the branching ratio and pendant vinyl groups such as the flexibility of the divinyl monomer, spacers between two vinyl groups and the overall divinyl concentrations and activities [29, 33, 34].

Injectable Hydrogel Fabrication and Rheological Analysis

Injectable hydrogels were prepared by Michael-type addition reaction between hyperbranched polyPEGDA and the commercially available thiolated hyaluronic acid (HA-SH, ESI.BIO) (**Scheme 1B**). The mechanism is described as a base-catalyzed reaction between the acrylate groups and thiolated anions under physiological condition [13]. The polymer solution (final concentration as 1%, 2.5% and 5.0 % (w/v)) was mixed gently with HA-SH solution at final concentration of 0.5% (w/v), and the gelation occured rapidly at room temperature. The gelation behaviors were further determined by oscillation rheology analysis with different conditions

(**Figure 5**). It was shown that the loss modulus (G") kept at a low level and the storage modulus (G') increased significantly, which suggested the gelation occurring. The gelling point was identified as the time point when G' started dramatically increasing, which in this case, all appeared within one to five minutes. Higher polymer concentration and temperature considerably speeded up the gelation as expected (**Figure 5A-B**). It was shown that even as low as 1% hyperbranched polyPEGDA polymer solution could form well stable hydrogel within 5 min at room temperature (20 ^{o}C); and around 1 min for the 2.5% polymer solution at body temperature (37 ^{o}C). The rapid gelation behavior due to the high amount of acrylate functional groups provides this system good potential for injectable hydrogel applications. Interestingly, at the molecular level, the differences of polymeric architecture caused by various $[M]_0$:$[CTA]_0$ ratio, as well as the polymer molecular weight did not seem to affect the gelling points at the macroscopical scale (**Figure 5C-D**). We assumed this was because the overall density of pendant vinyl groups in the solution were consistent in different groups which resulted in the same crosslinking speed via Michael-type addition reaction. On the other hand, it is worth to be noticed that in **Figure 5D**, even the higher molecular weight polyPEGDA (*M*n=13 kg/mol) was still controlled at the early stage of the reaction, in which the intermolecular coupling ratio was at a low level. It can be assumed that at the later stage of the reaction, the intermolecular hyperbranched polymer with large molecular weight can be considered as a gelling precursor which would significantly speed up the gelation [14].

Cell Behavior of Embedded rASCs in Injectable Hydrogels

To determine the biocompatibility of the injectable hydrogel from hyperbranched polyPEGDA and thiolated HA, certain polymer (entry 1 in Table 1, $[M]_0$:$[CTA]_0$ = 25/1, *M*n=13 kg/mol) was selected. Rat ASCs were embedded into the hydrogel by simply mixing the cell suspension and

gelling solution together, pipette onto a Teflon surface, and leave for 3-5 min to complete forming a hydrogel at room temperature. Then hydrogels were transferred into the culture medium for 3D culture up to two weeks. Cell viability, proliferation and metabolic activity were determined at each time point. As shown in **Figure 6**, LIVE/DEAD® (Molecular Probes®) assay indicated that over 85% of embedded rASCs kept alive in the hydrogels with different polymer concentrations (i.e. 2.5% and 5%) over two weeks. The unreacted vinyl groups with higher polymer concentrations in the hydrogel did not caused additional cytotoxicity to the embedded cells (**Figure S1 in supporting information**). We assumed this was because of the special hyperbranched structure of the polymer restricted the direct contact of the free vinyl groups and the embedded cells. Cell proliferation was observed under phase contrast microscope over time, and it was found that the embedded cells stop proliferating after about one week (**Figure S2 in supporting information**). Such result was also confirmed by PicoGreen® (Molecular Probes®) assay, in which the total DNA amount in the hydrogel significantly increased during the first week but discontinued since then ($n = 3$, $p < 0.05$, **Figure 7A**). Meantime, the cell metabolic activity remained at the same level over time and slightly decreased after 7 days, which was consisted with the results of the proliferation assessments (**Figure 7B**).

HA is a linear glycosaminoglycan that is one of the major components of the natural ECM. It has been widely studied for hydrogel tissue engineering and biomedical applications because of its good biocompatibility and highly hydrated nature [35, 36]. The molecular weight of natural HA can reach over 10^6 Da, but can be cleaved into small molecules by hyaluronidase [37]. It is interesting that HA with different molecular weight displays conflicting biological functions. For example, the high molecular HA inhibits the cell migration, proliferation, inflammatory and immune response; while the low molecular HA exhibit pro-inflammatory and pro-angiogenic behaviors

[38-40]. In this study, the molecular weight of the thiolated HA is around 200 kDa, which might cause pro-inflammatory effect in vivo and limit the embedded rASCs adhering, migrating and proliferating [41]. Generally, cells can interact with HA through cell-surface receptors such as cluster determinant 44 (CD44) and the receptor for hyaluronate-mediated motility (RHAMM), which play essential role in tissue organization and regeneration [2, 35]. However, lack of the cell adhesion molecules (CAMs), embedded cells can hardly spread and proliferate. Several CAMs have been used to improve the cell attachment on the HA hydrogels such as RGD peptide, and full-length proteins including collagen, fibronectin etc. [42-45]. On the other hand, HA hydrogels without additional adhesion modification showed remarkable advantages of controlling the stemness and differentiation of stem cells [46-48]. Here, to prove the concept of hydrogel microenvironment can be easily modified in our system which would significantly influence the cell morphology and behavior, fibrinogen (1% m/v in PBS) was simply mixed with gelling material to form a semi-interpenetrated polymer network (semi-IPN) structure. Thus fibrinogen as one of the most studied cell adhesion motifs can be encapsulated into the hydrogel, and the cell adhesion and spreading was significantly improved by fibrinogen after ten days (**Figure S3 in supporting information**). In addition, presented hydrogel system would be easily modified with any thiolated bioactive signals (e.g. peptide sequence, protein fragments, antibodies etc.) due to the large amount of the acrylate function groups on hyperbranched polyPEGDA polymer, which provide the promising potential of this system for tissue engineering and biomedical applications.

Conclusions

We demonstrated the synthesis of hyperbranched polyPEGDA homopolymer with high degree of acrylate functionality via one-step RAFT homopolymerization approach. RAFT agent significantly delayed the gelation, and well controlled molecular weight and polymeric architecture could be achieved by adjusting reaction time and monomer/CTA ratio. It was found that the lower monomer/CTA ratio decreased the intramolecular cyclization and increased the pendent vinyl functional group on the polymer chain. In addition, an injectable hydrogel can be formed by crosslinking this hyperbranched multifunctional polymer with a commercially available thiolated HA, and rapid gelation can be achieved under physiological conditions. 3D culture and cellular evaluation studies were performed with embedded rASCs, which indicated the present hydrogel system kept good cell viability and activities up to two weeks. Meantime, such hydrogel can be easily modified by adding extra bioactive molecules for certain application purpose. In summary, the present injectable hydrogel system from the hyperbranched multifunctional polyPEGDA homopolymers and thiolated HA showed significant potential for stem cell delivery in the field of tissue engineering and regeneration medical applications.

Experimental

Materials and Reagents

The monomers of poly(ethylene glycol) diacrylate (PEGDA, average M_n = 575 g/mol) were purchased from Sigma-Aldrich. 2,2′-Azobis(2-methylpropionitrile) (AIBN, Sigma-Aldrich, 98%) was used as an initiator of the polymerization. The chain transfer agent (CTA) of 2-cyanoprop-2-yl dithiobenzoate was synthesized according to published method [49]. Butanone (99%, HPLC grade, Aldrich), diethy ether (99%) and hexane (95%, Aldrich) were used as received. Thiolated hyaluronic acid (HA-SH, Glycosil®, ESI.BIO) was purchased from BioTime Inc., Alameda, CA.

Polymer Synthesis and Characterization

The hyperbranched polymer was synthesized by the homopolymerization of PEGDA via the reversible addition-fragmentation chain transfer (RAFT) approach. Briefly, the monomer of PEGDA (100/50/25 equiv) were dissolved in butanone at the monomer concentration of 0.4 mol/L in a two-necked round bottomed flask. Then initiator of AIBN (0.5 equiv) and CTA (1 equiv) were added in the flask, and the solution was purged with argon for 25 minutes to remove oxygen. The reaction was performed at 60 ^{o}C in an oil bath monitored by gel permeation chromatography (GPC). The polymerization was stopped by opening the flask and exposing the reaction to air. The monomer was removed by dropping the solution into a large excess of hexane/diethyl ether solution (1:2 v/v) and the solvent was removed by evaporation.

Molecular weights and molecular weight distributions (M_w/M_n) of the polymer samples were determined using GPC (Agilent PL-GPC50) with RI and viscosity detectors. The columns (30 cm PLgel Mixed-C, two in series) were eluted using chloroform and calibrated with poly(methyl methacrylate) (PMMA) standards. All calibrations and analysis were performed at 60 ^{o}C and a flow rate of 1 mL/min. ^{1}H NMR was carried out on a 300 MHz Bruker NMR with MestReNova processing software. The chemical shifts were referenced to the lock chloroform ($CDCl_3$, 7.26 p.p.m.). The branched ratio is defined as the branched PEGDA unit to all the unit, which can be calculated from the integral data (y and d labled in ^{1}H NMR spectrum in **Figure 3**) with the following equation (eqn 1):

$$Branch\ Ratio = 1 - \frac{\text{Linear PEGDA units}}{\text{All PEGDA units}} = 1 - \frac{\text{Integrals of y}}{\text{Integrals of d}/4} \quad \text{(eqn 1)}$$

^{13}C NMR was perfomed to confirm the polymer structure (**Figure S4 in supporting information**).

Injectable Hydrogels Fabrication and Rheological Assessments

To study the effects of different gelling condition, polymeric architecture and molecular weight influencing the hydrogel fabrication, hyperbranched polyPEGDA polymers were synthesized with different monomer to CTA ratio ($[M]_0$:$[CTA]_0$ = 25/50:1) and controlled molecular weight (M_n = 9 and 13 kg/mol and M_w/M_n around 1.8-2.0). The polymers were dissolved in PBS buffer (pH 7.4) and mixed gently by pipetting to the commercially available thiolated HA (HA-SH, ESI.BIO) that dissolved in degased dH_2O. The final concentrations of the polymer in gelling solution were 1%, 2.5% and 5% (w/v) and the HA-SH was 0.5% (w/v).

A Discovery HR-2 Rheometer (TA Instruments) with steel parallel-plate geometry (8 mm diameter) was used for rheological characterization of all the hydrogel samples. For real-time crosslinking rheological study, an oscillatory time sweep was performed at 20 and 37 ^oC respectively with different polymer samples. The gelling solutions were prepared as described above and transferred quickly on the sample plate to start the testing directly.

3D culture of rASCs in Injectable Hydrogels

Rat adipose-derived stem cells (rASCs) were extracted from rat adipose tissue and identified as previous reported [41]. For the present studies, only rASCs up to passage four was used. The selected hyperbranched polyPEGDA polymer ($[M]_0$:$[CTA]_0$ = 25:1, M_n=13 kg/mol) was dissolved in Dulbecco's Modified Eagle Medium (DMEM) medium, mixed with cell suspension and HA-SH by pipette, and quickly transferred 40 μL of the mixture onto a hydrophobic Teflon tape surface, leave at room temperature for 3-5 min for completely gel formation, and then transferred the hydrogels into a 24-well culture plate with 1 mL/well culture medium (DMEM with 10% FBS, 1% P/S). The final concentrations of polymer were 2.5% and 5% w/v; HA-SH as 0.5% w/v; and cells as 1 million/mL. Hydrogels were incubated at 37 ^oC in a humidified atmosphere of 5% CO_2 for 4, 7 and 14 days with medium change every 2-3 days.

Cell Viability, Metabolic Activity and Proliferation Assessments of the Embedded rASCs in the Hydrogels

For each time point, LIVE/DEAD® (Molecular Probes®), alamarBlue® (Invitrogen®) and PicoGreen® (Molecular Probes®) assays were used to determine the viability, metabolic activity and proliferation of the embedded rASCs respectively. LIVE/DEAD® and PicoGreen® assay were performed with the recommended procedure. For quantitative analysis of LIVE/DEAD® result, 9 micrographs with ×100 magnification were taken randomly from 3 hydrogel samples at each time point using an Olympus 1X41 inverted microscope. Live and dead cells were counted by using the software of ImagePro® Plus (Media Cybernetics, USA), and the cell viability was calculated by the ratio between the number of live cell and the total cell number in the field. For alamarBlue® assay, cell embedded hydrogels were incubated with 10% (v/v) alamarBlue® in complete culture medium for ten hours. The reduced alamarBlue® absorbance was determined by Varioskan Flash Plate Reader and calculated with recommended approach.

Acknowledgments.
This work was supported by grants from Science Foundation Ireland (SFI) under SFI-PI programme and Irish Research Council (IRC) under ELEVATE programme (ELEVATEPD/2014/61). We thank A. Gaffney and UCD Conway Imaging Core for kind help on embedded cell imaging.

SCHEME

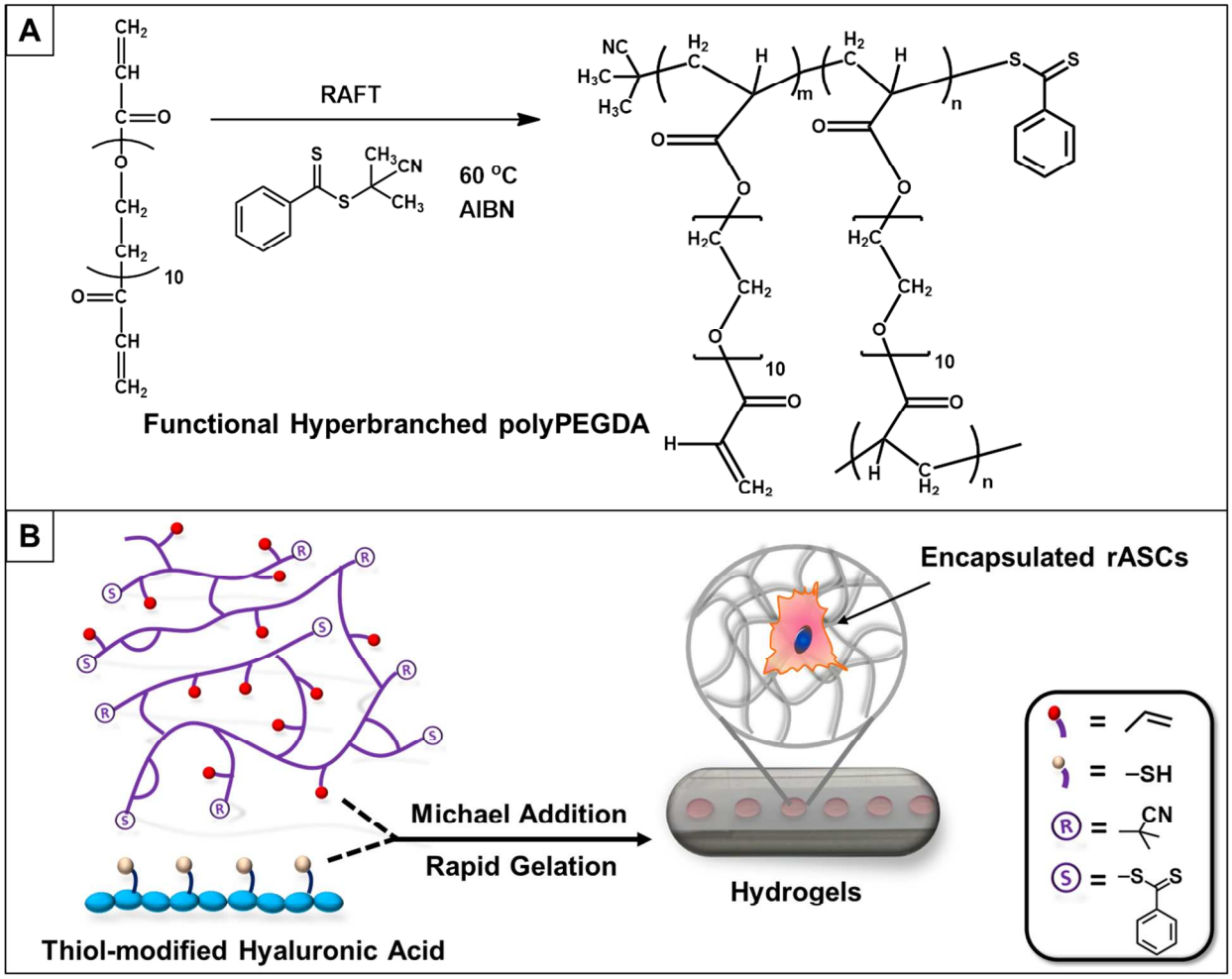

Scheme 1. (A) Hyperbranched acrylate functional polymer synthesized by homopolymerizing of poly(ethylene glycol) diacrylate (PEGDA) via Reversible Addition Fragmentation Chain Transfer (RAFT). (B) Schematic representation of the formation of the injectable hydrogels from hyperbranched functional polyPEGDA homopolymer and thiol-modified hyaluronic acid via Michael addition reaction, which encapsulating the rat adipose-derived stem cells (rASC).

FIGURES

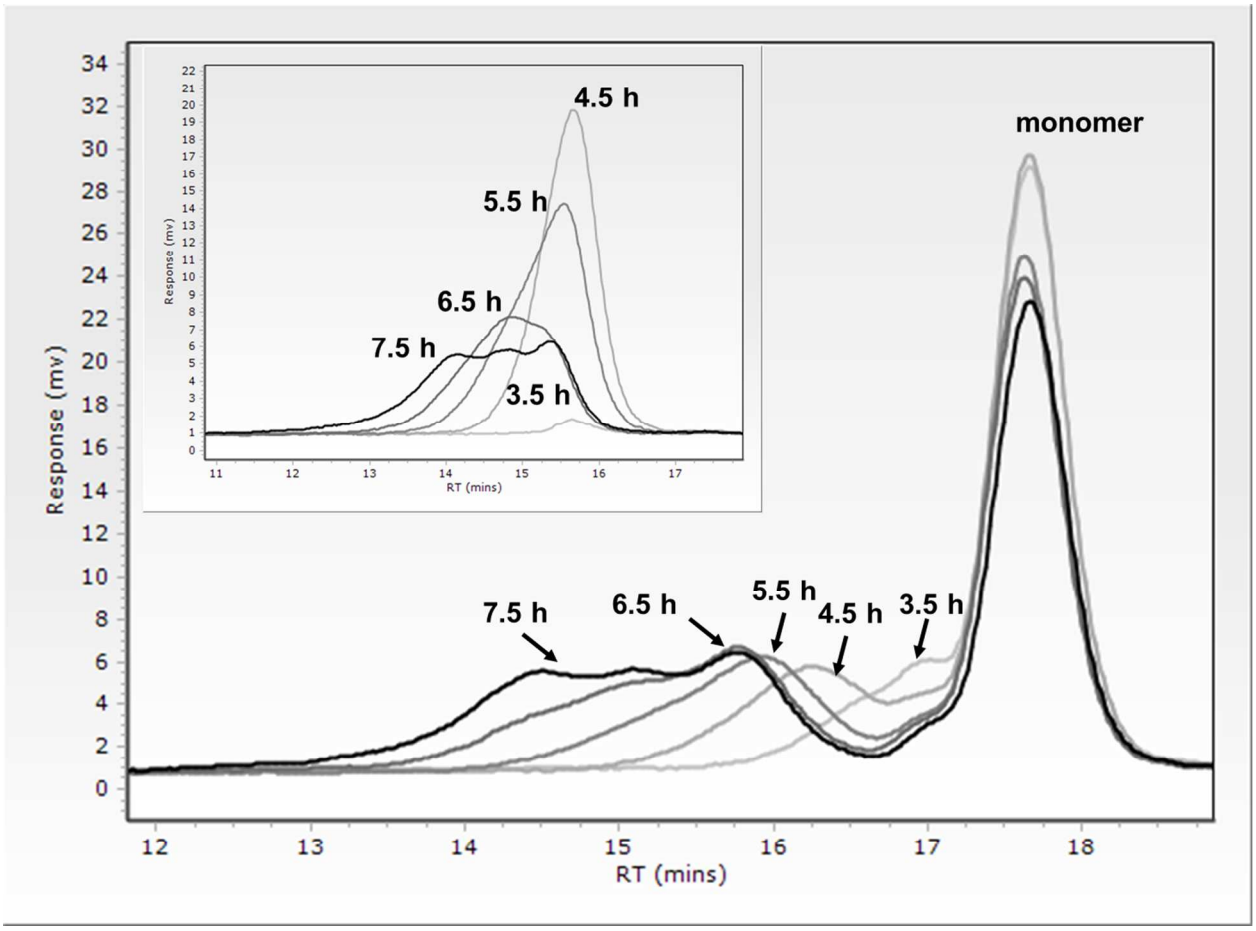

Figure 1. GPC traces of polyPEGDA (entry 1 in Table 1) by RAFT polymerization from RI detector. Increases in molecular weight and polydispersity with monomer conversion are observed. Insert shows the GPC traces of the purified samples by precipitation approach.

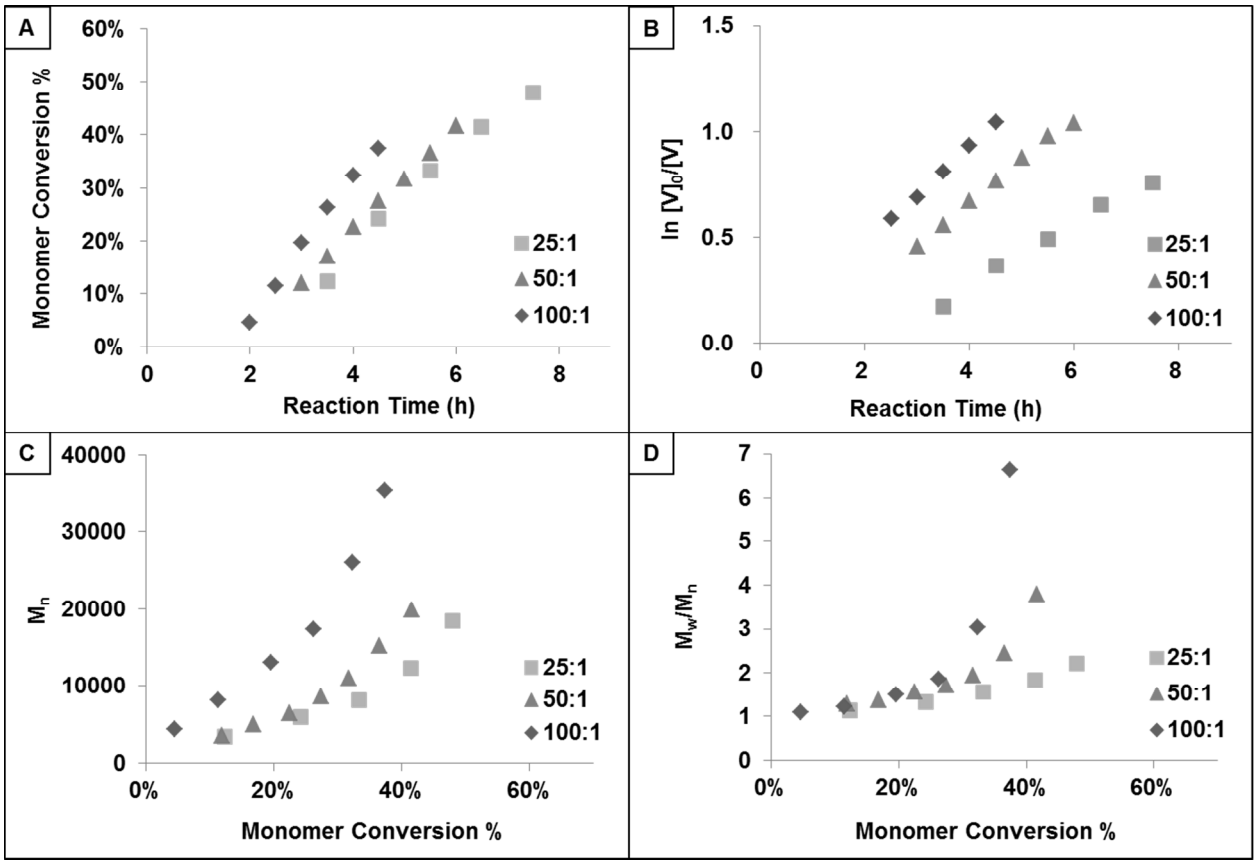

Figure 2. Kinetic plot of the RAFT polymerization of PEGDA with different monomer to CTA ratio ($[M]_0$:$[CTA]_0$ = 25/50/100:1) at 60 ^{o}C. Monomer concentration = 0.4 mol/L, [CTA]/[AIBN] = 2:1. Note: monomer conversion, number average molecular weight (M_n) and polydispersity index (M_w/M_n) were detected by GPC-RI, and In[V]/$[V]_0$ was calculated from ^{1}H NMR spectroscopy.

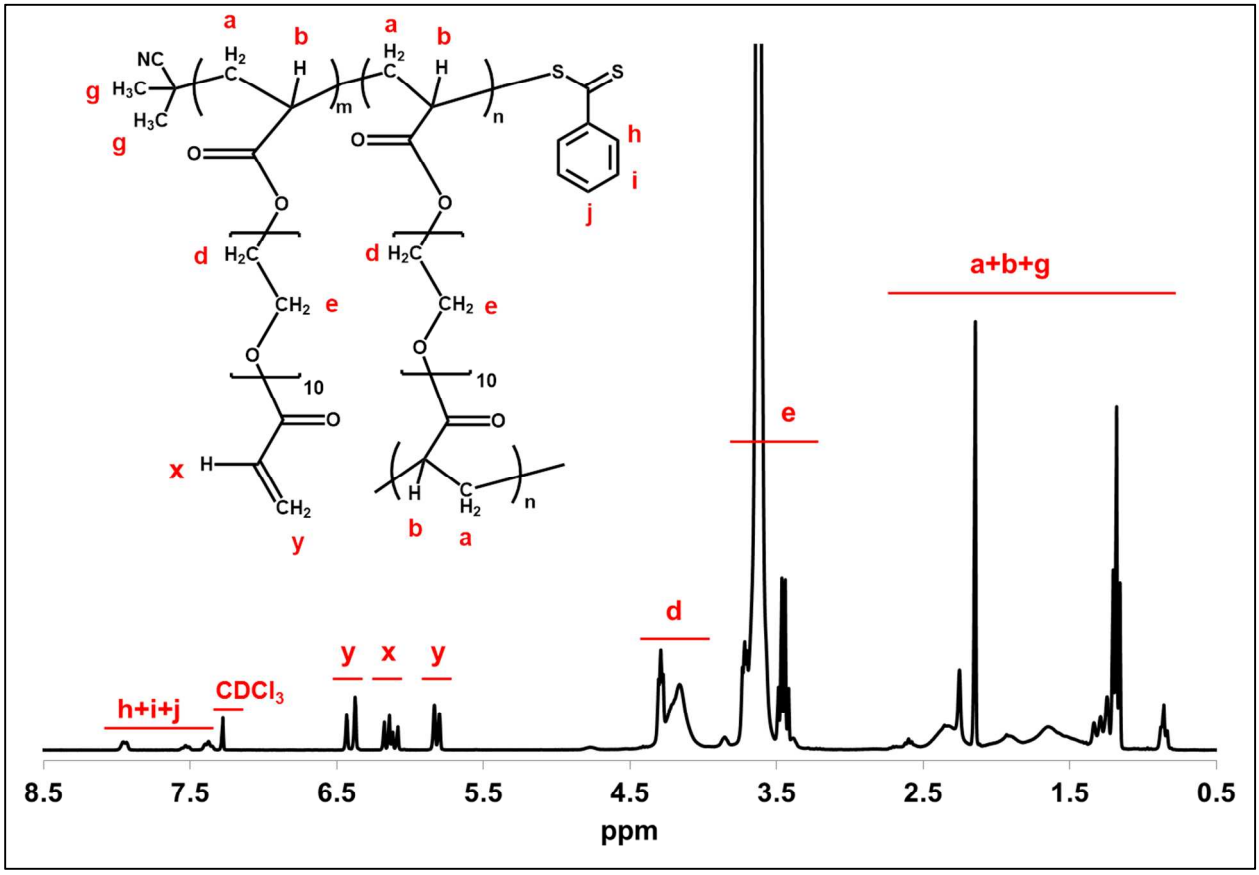

Figure 3. ^{1}H NMR for hyperbranched polyPEGDA (entry 1 in Table 1) in $CDCl_3$. The spectrum shows clearly the double bonds within the structure at the chemical shifts between 6.4 and 5.8 ppm.

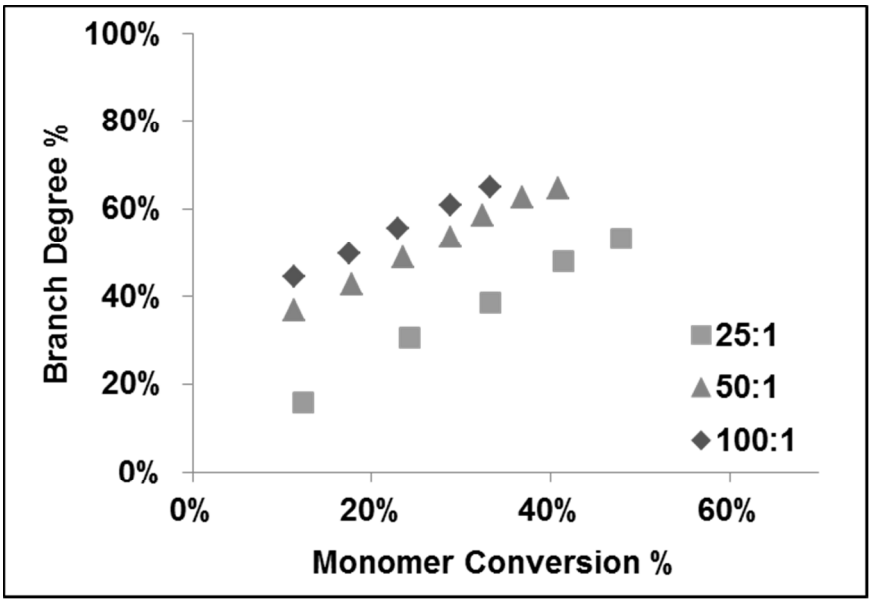

Figure 4. Branch degree - conversion plots for the RAFT homopolymerization of hyperbranched polyPEGDA with different monomer to CTA ratio ($[M]_0$:$[CTA]_0$ = 25/50/100:1) at 60 ^{o}C. Monomer concentration = 0.4 mol/L, [CTA]/[AIBN] = 2:1. Note: monomer conversion was detected by GPC-RI, and branch degree was calculated from ^{1}H NMR spectroscopy.

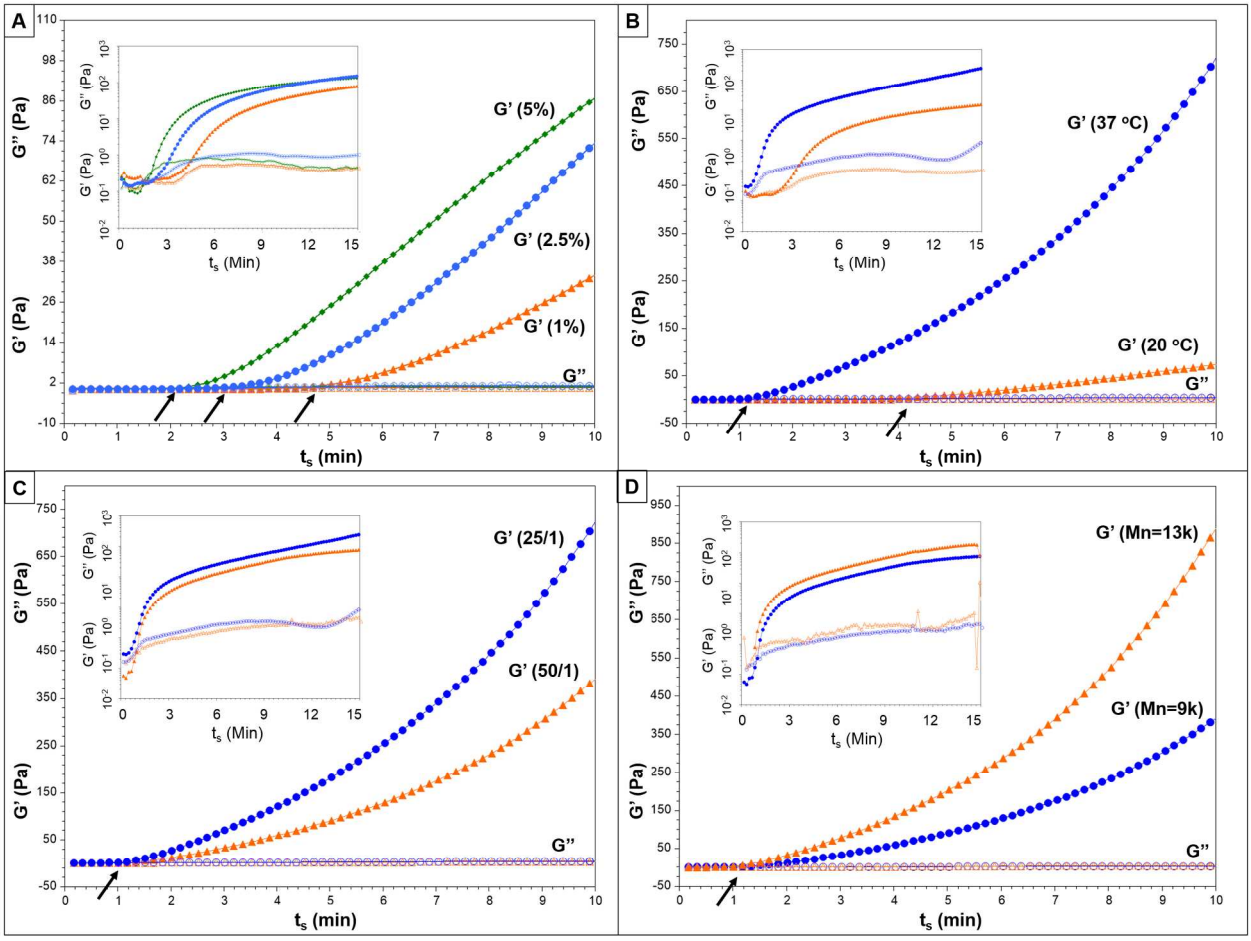

Figure 5. Real time chemical crosslinking rheological measurements of polyPEGDA homopolymers with thiolated HA (0.5% w/v). (A) Effect of polymer concentrations (entry 1 in Table 1, M_n = 9 kg/mol), performed at 20 °C. (B) Effect of temperature (entry 1 in Table 1, M_n = 9 kg/mol). (C) Effect of polymeric architectures (entry 1 and 2 in Table 1, M_n = 9 kg/mol, 2.5% w/v), performed at 37 °C. (D) Effect of polymer molecular weight (entry 1 in Table 1 M_n = 9 and 13 kg/mol, 2.5% w/v) performed at 37 °C. The arrows highlight the gelling points. G': storage modulus; G'': loss modulus. Inserts show the same data on a Log_{10} scale on G' and G''.

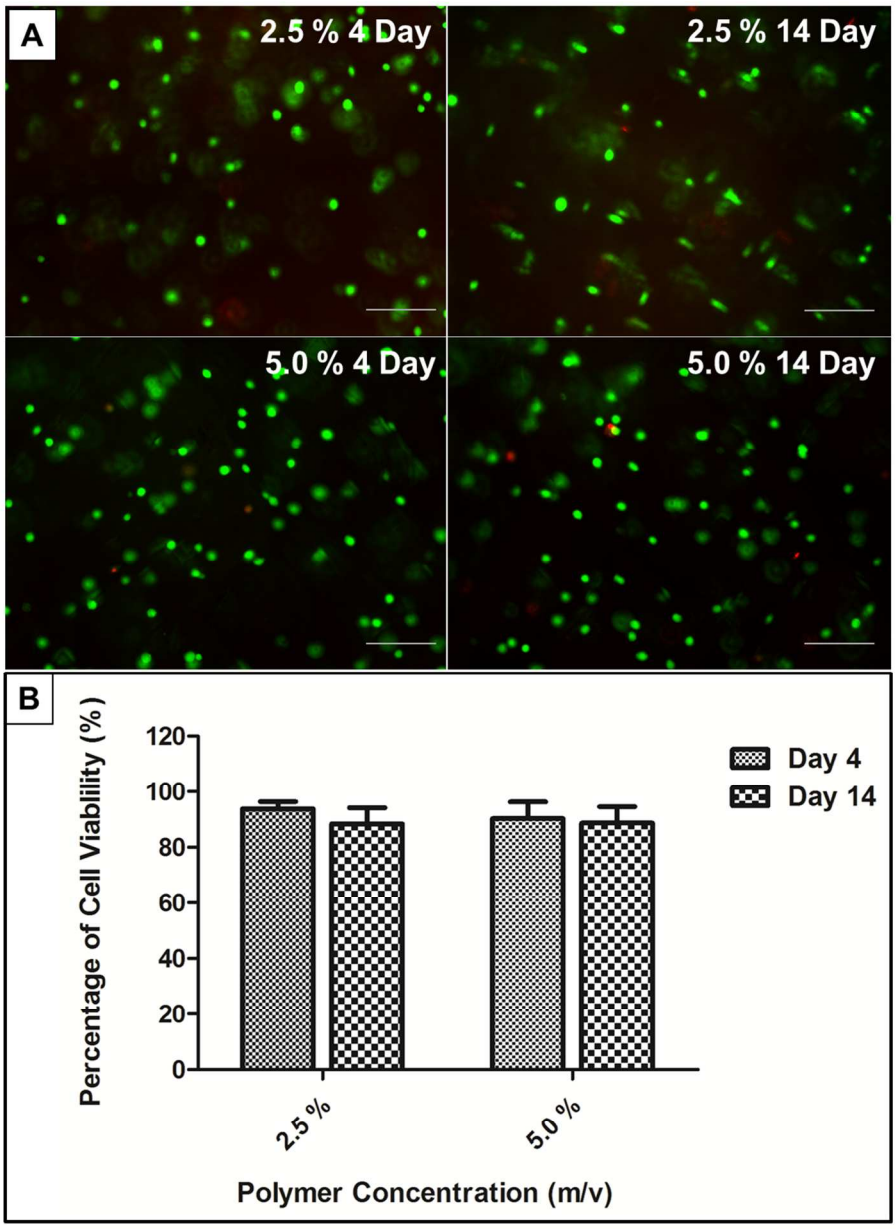

Figure 6. Cell viability analysis of embedded rASCs in the hydrogels by LIVE/DEAD® assay up to 14 days. (A) Representative fluorescent images of embedded rASCs. Calcein AM (green) stain for live cells and ethidum homodimer-1 (red) for dead cells (scale bars in all cases represent 100 μm). (B) Percentage of live cells to total cell number calculated from LIVE/DEAD® staining micrographs (mean ± SD,n= 3).

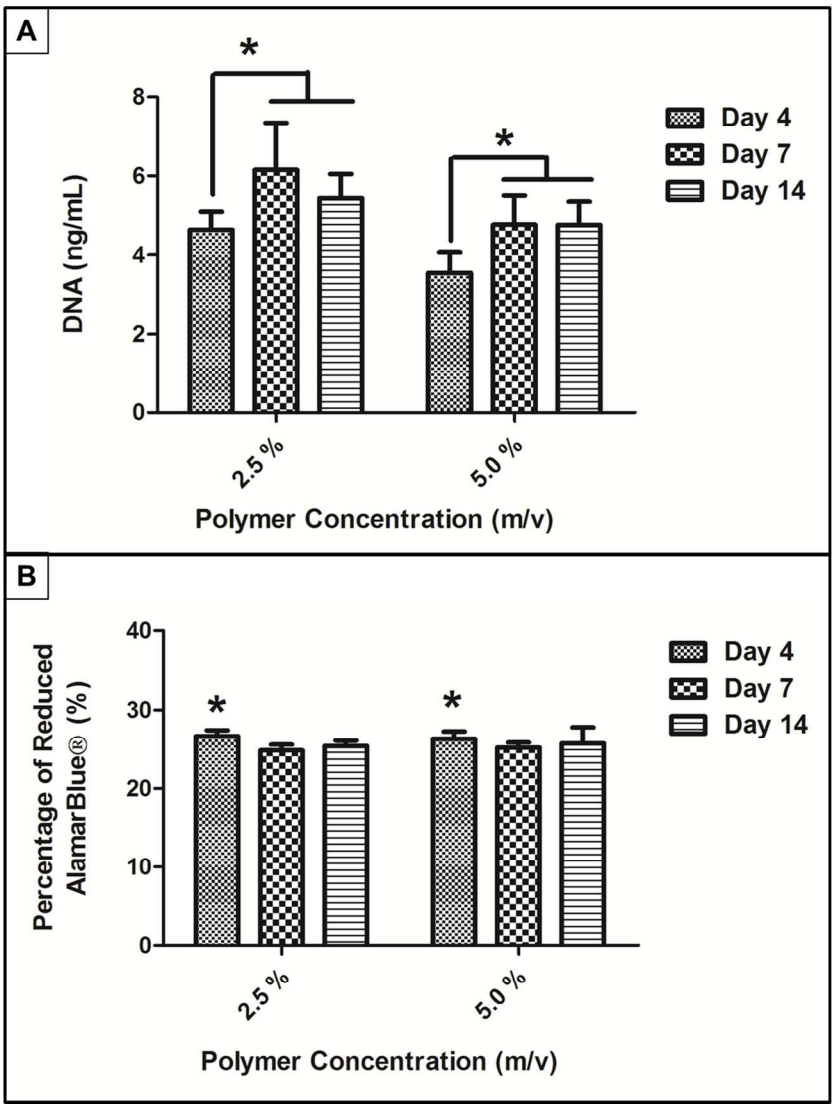

Figure 7. Cell proliferation and metabolic activity assessments of embedded rASCs in the hydrogels. (A) Cellular proliferation assay by PicoGreen® assay. Total DNA content in the hydrogel is significant increased for the first 7 days (mean ± SD, n = 3, $P < 0.05$). (B) Percentage of deduced alamarBlue® absorbance at 550 and 595 nm. Total cellular metabolic activity were reduced after 7 days (mean ± SD, n = 3, $P < 0.05$)

Table 1.

					Mn (Mw/Mn) [c]			Content(%) [e]	
entry	**[M]/[CTA]**	**sample #**	**RT [a]/h**	**conv. [b](%)**	**GPC-RI**	**GPC-Visco**	**α [d]**	**vinyl**	**Branch**
1	25/1	1	3.5	12	3.4 (1.14)	12.9 (1.39)	0.08	84	16
		2	4.5	24	6.0 (1.33)	15.3 (1.75)	0.18	69	31
		3	5.5	33	8.1 (1.56)	20.5 (2.24)	0.24	61	39
		4	6.5	41	12.3 (1.82)	26.0 (3.15)	0.28	52	48
		5	7.5	48	18.4 (2.21)	43.5 (4.49)	0.31	47	53
2	50/1	1	3.0	12	3.5 (1.27)	3.7 (1.40)	0.22	63	37
		2	3.5	17	4.9 (1.35)	4.8 (1.61)	0.24	57	43
		3	4.0	23	6.4 (1.55)	6.2 (1.79)	0.33	51	49
		4	4.5	27	8.6 (1.70)	8.9 (2.30)	0.32	46	54
		5	5.0	32	11.0 (1.93)	12.0 (3.40)	0.28	42	58
		6	5.5	37	15.2 (2.44)	18.0 (4.87)	0.27	38	62
		7	6.0	42	19.9 (3.79)	30.7 (8.64)	0.27	35	65
3	100/1	1	2.0	5	4.3 (1.09)	-	-	58	42
		2	2.5	11	8.0 (1.22)	12.4 (1.42)	0.19	55	45
		3	3.0	20	13.0 (1.49)	11.9 (1.87)	0.23	51	49
		4	3.5	26	17.4 (1.85)	14.1 (3.15)	0.25	44	56
		5	4.0	32	26.0 (3.03)	24.4 (6.40)	0.29	40	60
		6	4.5	37	35.4 (6.62)	41.1 (13.74)	0.25	35	65

[a] Reaction time. [b] Monomer conversion, estimated using peak areas for monomers and copolymers in GPC traces. [c] Number average molecular weight (M_n) and polydispersity index (M_w/M_n). [d] Mark-Houwink exponent (α). [e] Determined by ^{1}H NMR spectroscopy ($CDCl_3$). Polymerization conditions: 60 ^oC in butanone, [M] = 0.4 mol/L, [CTA]/[AIBN] = 2:1.

References

1. D. Seliktar, *Science*, 2012, **336**, 1124-1128.
2. M. Guvendiren and J. A. Burdick, *Current Opinion In Biotechnology*, 2013, **24**, 841-846.
3. J. A. Burdick and G. Vunjak-Novakovic, *Tissue Engineering Part A*, 2009, **15**, 205-219.
4. J. L. Drury and D. J. Mooney, *Biomaterials*, 2003, **24**, 4337-4351.
5. Y. Li, J. Rodrigues and H. Tomas, *Chemical Society Reviews*, 2012, **41**, 2193-2221.
6. J. H. Lee, H. B. Lee and J. D. Andrade, *Progress in Polymer Science*, 1995, **20**, 1043-1079.
7. N. A. Alcantar, E. S. Aydil and J. N. Israelachvili, *Journal of Biomedical Materials Research*, 2000, **51**, 343-351.
8. M. P. Lutolf and J. A. Hubbell, *Nature Biotechnology*, 2005, **23**, 47-55.
9. M. C. Cushing and K. S. Anseth, *Science*, 2007, **316**, 1133-1134.
10. M. P. Lutolf, *Nature Materials*, 2009, **8**, 451-453.
11. M. W. Tibbitt and K. S. Anseth, *Biotechnology and Bioengineering*, 2009, **103**, 655-663.
12. Y. Dong, P. Gunning, H. Cao, A. Mathew, B. Newland, A. O. Saeed, J. P. Magnusson, C. Alexander, H. Tai, A. Pandit and W. Wang, *Polymer Chemistry*, 2010, **1**, 827-830.
13. Y. Dong, A. O. Saeed, W. Hassan, C. Keigher, Y. Zheng, H. Tai, A. Pandit and W. Wang, *Macromolecular Rapid Communications*, 2012, **33**, 120-126.
14. R. Kennedy, W. Ul Hassan, A. Tochwin, T. Zhao, Y. Dong, Q. Wang, H. Tai and W. Wang, *Polymer Chemistry*, 2014, **5**, 1838-1842.
15. R. G. Alamo, W. W. Graessley, R. Krishnamoorti, D. J. Lohse, J. D. Londono, L. Mandelkern, F. C. Stehling and G. D. Wignall, *Macromolecules*, 1997, **30**, 561-566.
16. S. Carter, B. Hunt and S. Rimmer, *Macromolecules*, 2005, **38**, 4595-4603.
17. S. Peleshanko and V. V. Tsukruk, *Progress In Polymer Science*, 2008, **33**, 523-580.
18. D. Wang, T. Zhao, X. Zhu, D. Yan and W. Wang, *Chemical Society Reviews*, 2015, DOI: 10.1039/C4CS00229F.
19. P. J. Flory, *Journal Of the American Chemical Society*, 1952, **74**, 2718-2723.
20. C. J. Hawker, R. Lee and J. M. J. Frechet, *Journal Of the American Chemical Society*, 1991, **113**, 4583-4588.
21. J. M. J. Frechet, M. Henmi, I. Gitsov, S. Aoshima, M. R. Leduc and R. B. Grubbs, *Science*, 1995, **269**, 1080-1083.

22. A. H. E. Muller, D. Y. Yan and M. Wulkow, *Macromolecules*, 1997, **30**, 7015-7023.
23. E. Sato, I. Uehara, H. Horibe and A. Matsumoto, *Macromolecules*, 2014, **47**, 937-943.
24. N. O'Brien, A. McKee, D. C. Sherrington, A. T. Slark and A. Titterton, *Polymer*, 2000, **41**, 6027-6031.
25. F. Isaure, P. A. G. Cormack and D. C. Sherrington, *Journal Of Materials Chemistry*, 2003, **13**, 2701-2710.
26. F. Isaure, P. A. G. Cormack, S. Graham, D. C. Sherrington, S. P. Armes and V. Butun, *Chemical Communications*, 2004, 1138-1139.
27. I. Bannister, N. C. Billingham, S. P. Armes, S. P. Rannard and P. Findlay, *Macromolecules*, 2006, **39**, 7483-7492.
28. R. Baudry and D. C. Sherrington, *Macromolecules*, 2006, **39**, 5230-5237.
29. H. Mori and M. Tsukamoto, *Polymer*, 2011, **52**, 635-645.
30. K. Matyjaszewski, S. G. Gaynor, A. Kulfan and M. Podwika, *Macromolecules*, 1997, **30**, 5192-5194.
31. R. Wang, Y. Luo, B.-G. Li and S. Zhu, *Macromolecules*, 2009, **42**, 85-94.
32. M. L. Koh, D. Konkolewicz and S. Perrier, *Macromolecules*, 2011, **44**, 2715-2724.
33. M. Akiyama, K. Yoshida and H. Mori, *Polymer*, 2014, **55**, 813-823.
34. C.-D. Vo, J. Rosselgong, S. P. Armes and N. C. Billingham, *Macromolecules*, 2007, **40**, 7119-7125.
35. J. Lam, N. F. Truong and T. Segura, *Acta Biomaterialia*, 2014, **10**, 1571-1580.
36. M. N. Collins and C. Birkinshaw, *Carbohydrate Polymers*, 2013, **92**, 1262-1279.
37. K. S. Girish and K. Kemparaju, *Life Sciences*, 2007, **80**, 1921-1943.
38. D. C. West, I. N. Hampson, F. Arnold and S. Kumar, *Science*, 1985, **228**, 1324-1326.
39. D. C. West and S. Kumar, *Ciba Foundation Symposia*, 1989, **143**, 187-207.
40. A. J. Day and C. A. de la Motte, *Trends In Immunology*, 2005, **26**, 637-643.
41. Y. Dong, W. U. Hassan, R. Kennedy, U. Greiser, A. Pandit, Y. Garcia and W. Wang, *Acta biomaterialia*, 2014, **10**, 2076-2085.
42. Y. Lei, S. Gojgini, J. Lam and T. Segura, *Biomaterials*, 2011, **32**, 39-47.
43. D. L. Hern and J. A. Hubbell, *Journal Of Biomedical Materials Research*, 1998, **39**, 266-276.

44. C. N. Salinas and K. S. Anseth, *Journal Of Tissue Engineering And Regenerative Medicine*, 2008, **2**, 296-304.
45. B. V. Slaughter, S. S. Khurshid, O. Z. Fisher, A. Khademhosseini and N. A. Peppas, *Advanced Materials*, 2009, **21**, 3307-3329.
46. S. Gerecht, J. A. Burdick, L. S. Ferreira, S. A. Townsend, R. Langer and G. Vunjak-Novakovic, *Proceedings Of the National Academy Of Sciences Of the United States Of America*, 2007, **104**, 11298-11303.
47. C. Chung and J. A. Burdick, *Tissue Engineering Part A*, 2009, **15**, 243-254.
48. E. Dawson, G. Mapili, K. Erickson, S. Taqvi and K. Roy, *Advanced Drug Delivery Reviews*, 2008, **60**, 215-228.
49. M. Benaglia, E. Rizzardo, A. Alberti and M. Guerra, *Macromolecules*, 2005, **38**, 3129-3140.